Targeted gene disruption of methionine aminopeptidase 2 results in an embryonic gastrulation defect and endothelial cell growth arrest

Jing-Ruey J. Yeh*, Rong Ju*, Cathleen M. Brdlik*, Wenjun Zhang*, Yi Zhang*, Mary E. Matyskiela*, Joseph D. Shotwell*, and Craig M. Crews*†‡§

Departments of *Molecular, Cell, and Developmental Biology, †Pharmacology, and ‡Chemistry, Yale University, New Haven, CT 06520-8103

Edited by Judah Folkman, Harvard Medical School, Boston, MA, and approved May 10, 2006 (received for review December 31, 2005)

The antiangiogenic agent fumagillin (Fg) and its analog TNP-470 bind to intracellular metalloprotease methionine aminopeptidase-2 (MetAP-2) and inhibit endothelial cell growth in a p53-dependent manner. To confirm the role of MetAP-2 in endothelial cell proliferation and to validate it as a physiological target for the Fg class of antiangiogenic agents, we have generated a conditional MetAP-2 knockout mouse. Ubiquitous deletion of the MetAP-2 gene (*MAP2*) resulted in an early gastrulation defect, which is bypassed in double MetAP-2/p53 knockout embryos. Targeted deletion of *MAP2* specifically in the hemangioblast lineage resulted in abnormal vascular development, and these embryos die at the midsomite stage. In addition, knockdown of MetAP-2 using small interfering RNA or homologous recombination specifically suppresses the proliferation of cultured endothelial cells. Together, these results demonstrate an essential role for MetAP-2 in angiogenesis and indicate that MetAP-2 is responsible for the endothelial cell growth arrest induced by Fg and its derivatives.

angiogenesis | TNP-470

The methionine aminopeptidase (MetAPs) family of cytosolic metalloproteases are responsible for the cleavage of the initial methionine from the N termini of nascent proteins (1, 2). Eukaryotes express two forms of MetAPs, types 1 and 2, which possess similar *in vitro* substrate specificities. Removal of the N-terminal methionine by MetAP activity is important for subsequent N-terminal modifications, such as myristoylation (3) and acetylation (4). In addition, MetAP activity may affect protein stability according to the N-end rule proposed by Varshavsky and coworkers (5). It has been shown that MetAP function is essential for growth and survival of prokaryotes (which express only MetAP-1) and of the budding yeast *Saccharomyces cerevisiae* (6, 7). However, the physiological roles of MetAPs have not yet been identified in vertebrates.

MetAP-2 is specifically inhibited by TNP-470, a synthetic derivative of the *Aspergillus fumigatus* natural product fumagillin (Fg; see refs. 8 and 9). TNP-470 selectively inhibits endothelial cell growth *in vitro* with picomolar efficacy and has a potent antiangiogenic effect *in vivo* (10, 11). Because of the requirement of angiogenesis for solid tumor growth, MetAP-2 is currently being targeted with small-molecule inhibitors for anticancer and other angiogenesis-related diseases therapy, even though the mode of action of TNP-470 is not entirely clear (12–16). Several lines of evidence suggest that MetAP-2 is important for the antiangiogenic effect of TNP-470. First, we have recently demonstrated that an A362T variant of human MetAP-2 confers resistance to the cytostatic effect of a Fg analog in *MAP1*-null yeast (17). In addition, it has been shown that the ability of various Fg analogues to inhibit endothelial cell growth correlates with their MetAP-2 enzymatic inhibitory activity *in vitro* (9). However, a recent report using RNA interference (RNAi)-mediated MetAP-2 down-regulation contradicts our results and thus raises doubts about the role of MetAP-2 in mediating the antiangiogenic effect of TNP-470 (18). Thus, to validate MetAP-2 as an important therapeutic target, direct *in vivo* proof for the role of MetAP-2 in angiogenesis is needed.

To investigate the physiological roles of MetAP-2, we have created various MetAP-2-deficient mouse lines. Here we are able to identify a previously uncharacterized role for MetAP-2 in vertebrate development. We found that *MAP2*-null mouse embryos have reduced cell proliferation and show significant growth delay at embryonic day (E)6.5. These embryos do not start gastrulation or form mesoderm even at E8.5, indicating that MetAP-2 function is essential for embryonic development and survival at the initiation of gastrulation. Additionally, conditional knockout mouse embryos that lack MetAP-2 specifically in the hemangioblast lineage are able to develop past gastrulation to midsomite stage but later die because of poor vascular development. Thus, our results have provided *in vivo* evidence of the importance of MetAP-2 function in vasculogenesis. These *in vivo* results were corroborated in *in vitro* studies using RNAi and homologous recombination to reduce MetAP-2 protein levels, resulting in decreased endothelial cell proliferation. Taken together, our data confirm that MetAP-2 is indeed the cytostatic target of TNP-470 and is thus required for endothelial cell growth and angiogenesis.

Results

MetAP-2 Is Required for Murine Gastrulation. To analyze MetAP-2 function in embryogenesis, we generated a conditional knockout *MAP2* mouse strain (Fig. 1 *a* and *b*). Mice homozygous for the floxed allele $MAP2^{S/S}$ are viable, fertile, and show no abnormal phenotypes. Likewise, heterozygous-null $MAP2^{+/D}$ animals produced by breeding with transgenic mice expressing Cre recombinase under the control of the actin promoter (*ACTB-Cre*; see refs. 19 and 20) are also viable, fertile, and appear morphologically normal. However, upon intercrossing $MAP2^{+/D}$ mice, no homozygous-null $MAP2^{D/D}$ mice were born among 149 live offspring (Table 1, which is published as supporting information on the PNAS web site), indicating that loss of MetAP-2 resulted in embryonic lethality. Genotyping of the embryos dissected from timed heterozygous matings showed that the $MAP2^{D/D}$ embryos could be recovered until E8.5, although we found that $MAP2^{D/D}$ embryos were significantly smaller than their littermates at E7.5 (Fig. 1*c*). Immunostaining of anti-MetAP-2 antibody confirmed a great reduction of MetAP-2 protein levels in $MAP2^{D/D}$ embryos (Fig. 7, which is published as supporting information on the PNAS web site). Histological analysis of embryo sections also showed that *MAP2*

Conflict of interest statement: No conflicts declared.

This paper was submitted directly (Track II) to the PNAS office.

Freely available online through the PNAS open access option.

Abbreviations: Fg, fumagillin; HUVE, human umbilical vein endothelial; MetAP-2, methionine aminopeptidase 2; MPE, murine pulmonary endothelial; RNAi, RNA interference; PECAM, platelet endothelium cell adhesion molecule; shRNA, short hairpin RNA; HEK, human embryonic kidney; E*n*, embryonic day *n*.

§To whom correspondence should be addressed. E-mail: craig.crews@yale.edu.

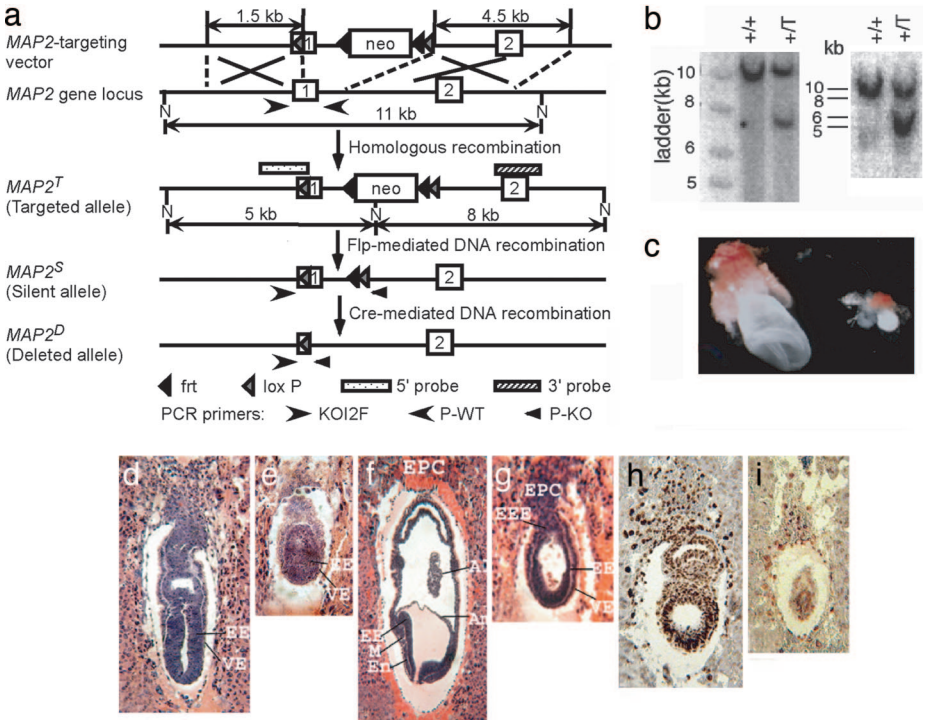

Fig. 1. Targeted modifications of the mouse *MAP2* locus and the embryonic phenotypes of *MAP2*-null mutants. (*a*) Derivation of various *MAP2* alleles. Two loxP sites were inserted into the 5′ UTR and the first intron of the *MetAP-2* gene. The neomycin resistance gene flanked by two frt sequences was also introduced into the intron. The neomycin resistance gene was then removed by crossing the targeted mice ($MAP2^{+/T}$) with transgenic mice expressing Flp under the control of the actin promoter (*ACTB-Flp*; see ref. 47), generating the floxed allele $MAP2^{S}$. Exons are depicted as open boxes, and thickened lines indicate the other genomic regions. Positions of the PCR primers and 5′ and 3′ probes for Southern blotting and the restriction enzyme site (N, NcoI) are shown. (*b*) Southern blot analysis of $MAP2^{+/T}$ mice. The probes used for NcoI digestion are the *MAP2* 5′ (*Right*) and 3′ (*Left*) probes as shown in *a*. (*c–g*) The embryonic phenotypes of *MAP2*-null mutants. (*c*) Whole-mount preparations of embryos at E7.5. The mutant embryo (*Right*) is much smaller than its wild-type littermate (*Left*). (*d–g*) Hematoxylin/eosin-stained sagittal sections. (*d*) E6.5 wild-type embryo at the egg-cylinder stage. (*e*) E6.5 mutant embryo. The embryo is smaller and disorganized. (*f*) E7.5 wild-type embryo at the primitive-streak stage. The embryo is well advanced in gastrulation. (*g*) E7.5 mutant embryo. The embryo is small and has developed to the egg-cylinder stage but has not begun gastrulation. (*h* and *i*) *In vivo* BrdUrd incorporation of E7.5 embryos revealing proliferating cells. (*h*) Strongly BrdUrd-positive nuclei can be seen throughout the wild-type embryo. (*i*) Fewer BrdUrd-positive cells with much weaker signals are seen, especially in the epiblast of the *MetAP-2* mutant embryo. AL, allantois; AM, amnion; EE, embryonic endoderm; EEE, extraembryonic ectoderm; En, endoderm; EPC, ectoplacental cone; M, mesoderm; and VE, visceral endoderm.

homozygous mutants were consistently reduced in size compared with their wild-type or heterozygous littermates by E6.5 (Fig. 1 *d* and *e*). At E7.5, instead of being in midgastrulation stage as were the control embryos, $MAP2^{D/D}$ embryos appeared to be in the egg-cylinder stage (E6.0; Fig. 1 *f* and *g*). $MAP2^{D/D}$ embryos did not develop beyond the egg-cylinder stage by E8.5 and were subsequently resorbed (Fig. 8, which is published as supporting information on the PNAS web site). However, at E7.5, $MAP2^{D/D}$ embryos showed normal development of ectoplacental cones and maternal–embryonic interface and well defined extraembryonic and embryonic ectoderm, as well as visceral and parietal endoderm. The only obvious defect of these embryos was the lack of distinct mesoderm, indicating the failure to start gastrulation (Fig. 1 *f* and *g*).

Because $MAP2^{D/D}$ mutants showed evident growth delay by E6.5, we investigated the effect of *MAP2* disruption on cell proliferation by *in vivo* BrdU incorporation. As compared with control embryos (Fig. 1*h*), anti-BrdU staining in mutant epiblasts was much weaker, and the number of stained nuclei was diminished (Fig. 1*i*), indicating decreased cell proliferation. Unexpectedly, we found that the *in vitro* growth of both the inner cell mass and trophoblast from $MAP2^{D/D}$ blastocysts is comparable to that from wild-type blastocysts, suggesting that MetAP-2 is not required for cell survival or proliferation *per se* in early postimplanted mouse embryos (Fig. 9, which is published as supporting information on the PNAS web site). Because the decreased cell proliferation in $MAP2^{D/D}$ mutants is specific to the pregastrulation stage, when cell migration and rapid cell proliferation take place, we postulated that MetAP-2 may be involved in morphogenesis during gastrulation. The defects of cell movements in $MAP2^{D/D}$ embryos during gastrulation could then induce embryonic cell growth arrest.

To confirm that $MAP2^{D/D}$ embryos could not initiate gastrulation, we examined the expression of several early gastrulation markers at E7.5 by RNA *in situ* hybridization. Although we detected a strong expression of the early mesoderm marker *T* (*Brachyury*) gene (21) in the primitive streak of the control embryos, we did not detect any T gene expression in $MAP2^{D/D}$ embryos (Fig. 2 *a* and *b*). *Otx2* is a homeodomain-containing transcription factor that is initially expressed throughout epiblast and visceral endoderm, but whose expression becomes restricted to the anterior ectoderm and the external layer after gastrulation (22). Although we observed normal Otx2 expression in the control embryos, $MAP2^{D/D}$ embryos displayed a weak and uniform staining throughout the entire embryos (Fig. 2 *c* and *d*). Another gastrulation marker, *Bmp4*, was expressed in extraembryonic mesoderm of amnion and allantois of the control E7.5 embryos, as reported (ref. 23; see also Fig. 2*e*). However, no Bmp4 expression was detected in $MAP2^{D/D}$ embryos (Fig. 2*f*). Finally, although the expression of the mouse *Cer1* gene, a member of the cysteine knot cytokine family, was localized in the anterior neural ectoderm and somatic mesoderm of the control E7.5 embryos (24), *Cer1* expression was weak and showed no distinct pattern in $MAP2^{D/D}$ embryos (Fig. 2 *g* and *h*). Collectively, these data indicate the requirement of MetAP-2 in vertebrate

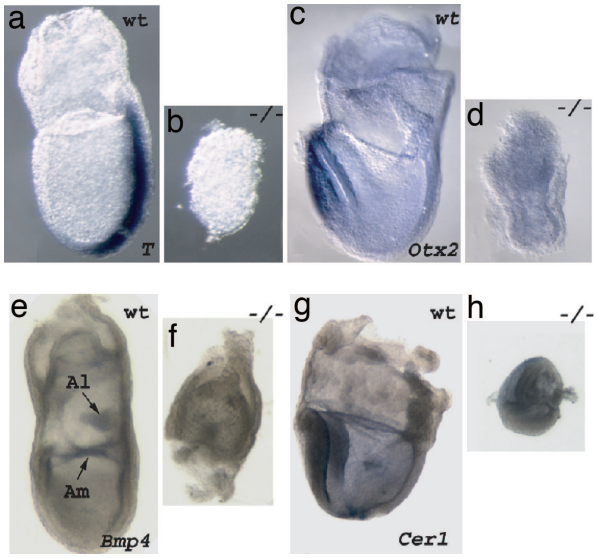

Fig. 2. *In situ* hybridization analysis of *T* (*a* and *b*), *Otx2* (*c* and *d*), *Bmp4* (*e* and *f*), and *Cer1* (*g* and *h*) expression in E7.5 embryos. *MAP2* wild-type (wt) and mutant (−/−) embryos are shown at the same magnification. Mesometrial pole is toward the top, and posterior is to the right. Al, allantois; Am, amnion membrane.

embryonic development, whereby failure of its expression prevents gastrulation.

Loss of p53 Rescues Early Gastrulation Arrest of MetAP-2-Deficient Embryos. Previous work from our lab and others has demonstrated that TNP-470 inhibits endothelial cell proliferation by means of the p53 and $p21^{CIP/WAF}$ pathway (25, 26). To determine whether loss of MetAP-2 induces p53 expression *in vivo*, we first examined p53 expression in control and *MAP2*-null embryos by immunohistochemical staining. As shown in Fig. 3 *a* and *b*, whereas p53 expression was very weak in the control embryos at E7.5, high levels of p53 protein were detected in epiblasts and extraembryonic tissues of the same stage $MAP2^{D/D}$ embryos. Thus, inhibition of

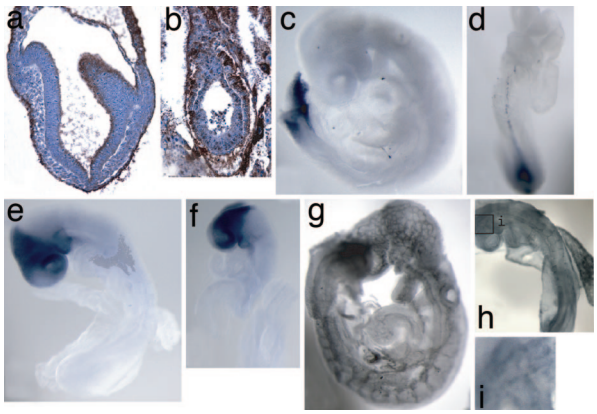

Fig. 3. Loss of p53 rescues early gastrulation arrest in MAP2-deficient embryos. (*a* and *b*) Immunohistochemical staining of p53 on a sagittal section of E7.5 control embryo (*a*) and *MAP2* mutant embryo (*b*). p53 protein was dark-brown nuclear stained, and the sections were counterstained with hematoxylin (blue). (*c–f*) RNA *in situ* hybridization of *T* (*c* and *d*) and *Otx2* (*e* and *f*) gene in $MAP2^{+/D}$ $p53^{-/-}$ (*c* and *e*) and $MAP2^{D/D}$ $p53^{-/-}$ embryos (*d* and *f*) at E9.5. (*g–i*) Whole-mount PECAM staining of E9.5 $MAP2^{+/D}$ $p53^{-/-}$ (*g*) and $MAP2^{D/D}$ $p53^{-/-}$ (*h*) embryos. (*i*) Capillaries in the head of a $MAP2^{D/D}$ $p53^{-/-}$ embryo (*h*).

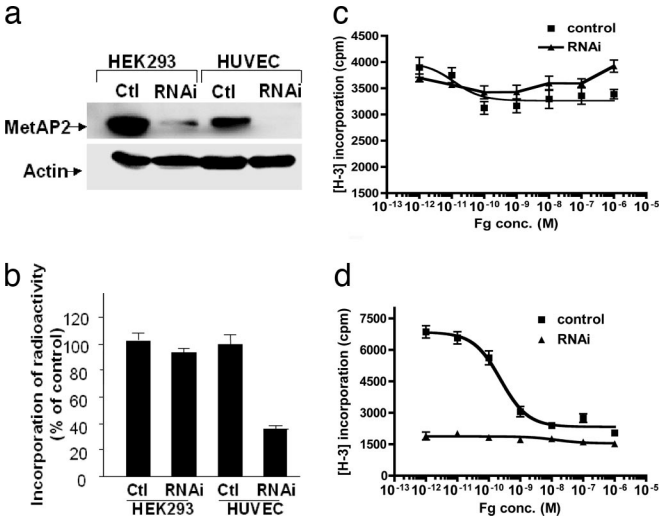

Fig. 4. RNAi-mediated MetAP-2 knockdown. (*a*) Western blot analysis of MetAP-2 in HEK293 and HUVE cells. Twenty micrograms of cell lysate was fractionated on SDS/PAGE and immunoblotted with anti-MetAP-2 or antiactin antibodies. (*b*) The effect of MetAP-2 knockdown by RNAi on cell proliferation assessed by [^{3}H]thymidine incorporation. (*c*) Fg sensitivity of HEK293 cells with RNAi depletion of MetAP-2. (*d*) Fg sensitivity of HUVE cells with RNAi depletion of MetAP-2. Cell proliferation and Fg sensitivity were determined as described in *Materials and Methods*. Ctl, control (empty vector). Results are presented as the mean and standard deviation of six separate samples.

MetAP-2 function results in elevated p53 expression in pregastrulation mouse embryos.

Next, we tested whether deletion of the *p53* gene could rescue the growth arrest observed in *MAP2* mutant embryos. We introduced the $MAP2^{D}$ mutation into a *p53*-null genetic background (27). Among 104 pups from the $MAP2^{+/D}$ $p53^{+/-}$ and $MAP2^{+/D}$ $p53^{-/-}$ crosses, there were no live $MAP2^{D/D}$ $p53^{-/-}$ animals (the expected number of $MAP2^{D/D}$ $p53^{-/-}$ animals was 13). Examination of embryos during gestation, however, showed that $MAP2^{D/D}$ $p53^{-/-}$ embryos were able to develop past gastrulation and survive until E9.5. These embryos then became necrotic. Six of seven $MAP2^{D/D}$ $p53^{-/-}$ embryos harvested at E9.5 were smaller than their wild-type or heterozygous *MAP2* littermates but had developed an anterior–posterior pattern with a head, trunk, and tail region. In agreement with this observation, we were able to detect *T* gene and *Otx2* gene expression in notochord mesoderm and telecephalon of these embryos, respectively (Fig. 3 *c–f*). The remaining one $MAP2^{D/D}$ $p53^{-/-}$ embryo and all of the $MAP2^{D/D}$ littermates in p53 heterozygous background did not progress past gastrulation (data not shown). Whole-mount staining with anti-platelet endothelium cell adhesion molecule (PECAM) antibody also showed that $MAP2^{D/D}$ $p53^{-/-}$ embryos formed an initial vascular network, especially in the brain, although they were less complex compared with $MAP2^{+/D}$ $p53^{+/-}$ or $MAP2^{+/D}$ $p53^{-/-}$ littermates (Fig. 3 *g–i*).

MetAP-2 Is Required for Endothelial Cell Proliferation. To test directly whether MetAP-2 is the target of the Fg family of antiangiogenic compounds, we performed experiments to deplete cells of MetAP-2 and to examine what effect this depletion has on the growth of endothelial cells. We first designed a series of short hairpin RNA (shRNA) constructs to knock down MetAP-2 protein levels in human umbilical vein endothelial (HUVE) cells and human embryonic kidney (HEK)293 cells, a HEK epithelial cell line that is not sensitive to Fg. One particular shRNA construct targeting the 3′ UTR of the human *MAP2* gene proved most effective. This sequence differs from the sequence used previously to target MetAP-2 (18). Fig. 4*a* shows that in both HEK293 and HUVE cells, this shRNA construct is able to inhibit the majority of

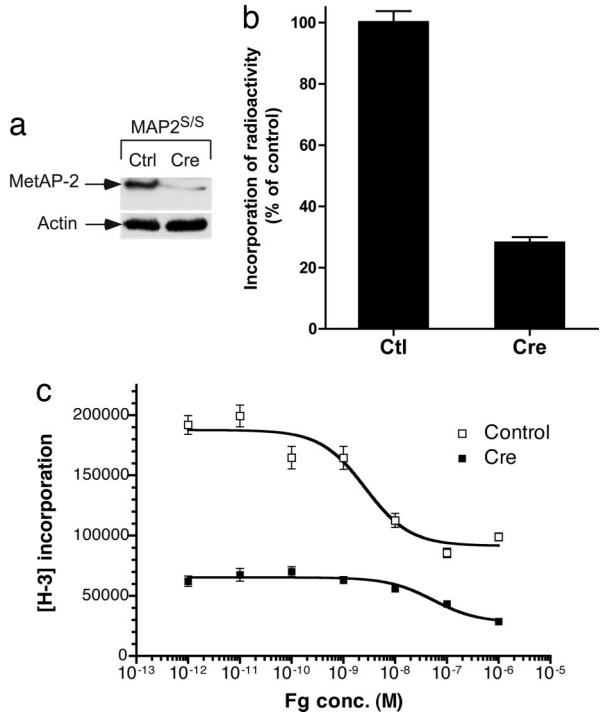

Fig. 5. The *MAP2* gene knockout in MPE cells. (*a*) Western blot analysis of MetAP-2 in MPE cells. Ten micrograms of cell lysate was run out by SDS/PAGE and immunoblotted with anti-MetAP-2 or antiactin antibodies, as indicated. (*b*) The effect of *MAP2* knockout on MPE cell proliferation as assessed by [^{3}H]thymidine incorporation. (*c*) Fg sensitivity of MPE cells with excised *MAP2* alleles. Ctl, control (empty vector). Results are presented as the mean and standard deviation of six samples.

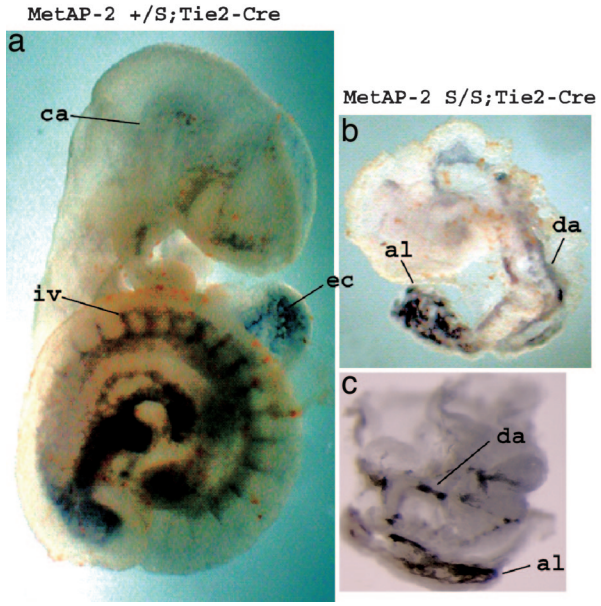

Fig. 6. Whole-mount PECAM staining of *MAP2* hemangioblast-specific knockout embryos. (*a*) A normal-looking E9.5 heterozygous embryo. Staining can be observed in endocardium, dorsal aorta, intersomitic vessels, and capillaries. (*b* and *c*) At E9.5, homozygous mutant embryos are growth-retarded and necrotic. Staining can be observed in the allantois and the poorly developed dorsal aorta. ec, endocardium; da, dorsal aorta; iv, intersomitic vessels; ca, capillaries; and al, allantois.

MetAP-2 protein expression relative to that in control cells. MetAP-2 levels were almost undetectable when this particular shRNA was expressed in HUVE cells. The persistent low level of MetAP-2 expression in HEK293 cells after RNAi may be due to the higher endogenous MetAP-2 expression compared with that in HUVE cells (Fig. 4*a*). To evaluate the growth effect of MetAP-2 knockdown, we performed [^{3}H]thymidine uptake assays on these cells. As shown in Fig. 4*b*, the growth of HUVE cells expressing MetAP-2 shRNA was inhibited by ≈70% as compared with 10% in HEK293 cells expressing MetAP-2 shRNA. These data suggest that loss of MetAP-2 results in an endothelial-specific growth inhibition. In addition, although HEK293 is resistant to the cytostatic effect of Fg at doses up to 1 μM, the maximum growth inhibition of HUVE cells can be achieved at 10 nM Fg (Fig. 4 *c* and *d*). However, Fg has almost no effect on the growth of MetAP-2 knockdown HUVE cells (Fig. 4*d*). Meanwhile, the growth of MetAP-2 knockdown HUVE cells is comparable to the growth of control HUVE cells under the maximum Fg-mediated growth inhibition (Fig. 4*d*). The finding strongly suggests that MetAP-2 is the target of Fg for its ability to specifically arrest endothelial cell growth.

Because of the discrepancy between our MetAP-2 RNAi results and those of a previous report (18), we further confirmed the finding by using our unique *MAP2* targeting mice. Isolated pulmonary endothelial cells from the floxed *MAP2* conditional knockout mouse line ($MAP2^{S/S}$) were infected with retroviruses expressing the Cre recombinase gene and selected for antibiotic resistance. The depletion of MetAP-2 protein in these cells was confirmed by Western blot analysis (Fig. 5*a*). Relative to MetAP-2 protein levels in $MAP2^{S/S}$ cells infected with the viral vector lacking an insert (control), MetAP-2 levels in $MAP2^{S/S}$ cells expressing Cre recombinase were dramatically reduced. Slightly detectable levels of MetAP-2 persist after Cre expression, which may be attributed to incomplete elimination of uninfected cells or incomplete DNA recombination. Despite the residual MetAP-2 levels, the proliferation of *MAP2* knockout murine pulmonary endothelial (MPE) cells is dramatically decreased to <30% of that of control cells (Fig. 5*b*). Furthermore, although 10 nM Fg exerts almost maximum inhibition on the growth of control MPE cells, at this concentration, it had almost no effect on the growth of *MAP2* knockout MPE cells (Fig. 5*c*). However, at concentrations >10 nM, Fg started to inhibit the growth of *MAP2* knockout MPE cells. This growth inhibition may be due to the cytotoxicity of Fg at concentrations above the cytostatic doses, because that has been observed with TNP-470 (10), or it is possible that the cells that continue to proliferate after partial MetAP-2 knockdown have lower Fg sensitivity than wild-type MPE cells. We also found that the degree of reduction in the growth of MPE cells as a result of MetAP-2 knockdown is comparable to the maximum Fg-mediated growth inhibition in control MPE cells. Thus, data obtained from the genetically engineered MPE cells corroborate our RNAi results, indicating that MetAP-2 is the cytostatic target of Fg.

MetAP-2 Is Required for Murine Vasculogenesis. Because $MAP2^{D/D}$ mutants die before vasculogenesis begins, to address the *in vivo* role of MetAP-2 in murine vascular development, we specifically deleted *MAP2* in hemangioblasts, the progenitors of both hematopoietic and endothelial cells. To do so, we crossed floxed *MAP2* mice ($MAP2^{S/S}$) with *TIE2-Cre* transgenic mice. It has been shown that the *TIE2* promoter is activated beginning at E7.5 in hemangioblasts (28). Genotypic analysis of 79 live offspring from $MAP2^{S/S}$ and $MAP2^{+/S:TIE2\text{-}Cre}$ crosses indicated that $MAP2^{S/S:TIE2\text{-}Cre}$ animals were not viable (19 $MAP2^{S/S:TIE2\text{-}Cre}$ animals were expected). However, we found that $MAP2^{S/S:TIE2\text{-}Cre}$ embryos were able to survive past early gestation stage and could be recovered as late as E10.5. These mutant embryos developed to midsomite stage (E8.5) but then became arrested and necrotic at E9.5 (Fig. 6 *b* and *c*). At E9.5, $MAP2^{S/S:TIE2\text{-}Cre}$ embryos appeared disorganized and smaller than

their $MAP2^{+/S:TIE2\text{-}Cre}$ or $MAP2^{S/S}$ littermates. Similar phenotypes have also been found in mice homozygous-null for VEGF or a VEGF receptor (*Flt-1*) (29, 30). Whole-mount staining for the vascular cell marker PECAM revealed that $MAP2^{S/S:TIE2\text{-}Cre}$ embryos contained significantly less PECAM-positive endothelial cells as compared with their phenotypically wild-type $MAP2^{+/S:TIE2\text{-}Cre}$ littermates (Fig. 6). Additionally, the cells that were PECAM-positive in the mutant embryos displayed a relatively diffuse staining pattern. The blood vessels, such as dorsal aorta, intersomitic vessels, and small capillary plexus in $MAP2^{S/S:TIE2\text{-}Cre}$ embryos, were either poorly developed or failed to be distinguished. Thus, vascular development became arrested soon after the *MAP2* gene was disrupted in endothelial cells. Our data clearly indicate that MetAP-2 is essential for the development of the endothelial lineage and vasculogenesis in early-stage murine embryos.

Discussion

A Role for MetAP-2 in Gastrulation. We previously demonstrated that MetAP-2 is the target of the potent antiangiogenic compound Fg (8), which selectively inhibits the *in vitro* growth of endothelial cells (31). There are two MetAP family members, MetAP-1 and -2, in eukaryotes. Together, they affect many cellular processes by means of N-terminal modifications. Even though the enzymatic activities of MetAPs are essential for cell survival, it has been shown that MetAP-1 can generally compensate MetAP-2 deficiency and vice versa. For example, yeast cells lacking either the *MAP1* or the *MAP2* gene are viable, but double-null yeast cells are lethal (7). In addition, global protein myristoylation is unaffected in endothelial cells treated with TNP-470 (32). Moreover, it is found that both MetAP-1 and -2 are expressed in Fg-sensitive and -resistant cells (33). Thus, it is difficult to parse the physiological roles of these two MetAPs.

To explore the *in vivo* role of MetAP-2, we generated *MAP2* homozygous-null mice, which displayed an embryonic lethal phenotype. *MAP2* mutant embryos fail to gastrulate, indicating that MetAP-2 function is essential for embryonic development at gastrulation. It is fairly surprising that deletion of the *MAP2* gene causes such early embryonic lethality. In yeast, deletion of the *MAP1* gene results in slow growth phenotype, whereas deletion of the *MAP2* gene has a negligible effect on growth (7). We also found that, although MetAP-2 deficiency resulted in reduced cell proliferation of mouse embryos at E7.5, it did not affect the *in vitro* growth of blastocysts in cell culture. Thus, MetAP-2 is not required for embryonic cell proliferation *per se* but rather is likely involved in other essential processes during gastrulation, such as cell polarity and migration, upon which subsequent cell survival and proliferation would largely depend. It has been shown in *Drosophila* that flies with a *MAP2* null allele do not survive to adulthood, whereas partial reduction in *MAP2* function leads to very specific phenotypes in the eyes and wings of surviving adult flies, reminiscent of perturbation of Wnt signaling pathway (34). Recent work from our laboratory has demonstrated a role for MetAP-2 in noncanonical Wnt signaling (Y.Z., J.-R.J.Y., A. Mara, J. F. Hines, P. Cirone, *et al.*, unpublished data), which is critical for morphogenetic movements and cell separation during vertebrate gastrulation (35). The finding is consistent with the observed murine gastrulation defect in the *MAP2*-null mice reported here.

A p53-Dependent Checkpoint in Gastrulation. Our laboratory and others have shown that the Fg class of antiangiogenic compounds mediate their cytostatic activities by means of a p53-dependent mechanism (25, 26). We find that *MAP2*-null mouse embryos have elevated p53 expression, and that deletion of the *p53* gene rescues the pregastrulation arrest observed in *MAP2*-null embryos prolonging survival until E9.5. Similarly, earlier reports have shown that loss of p53 can partially rescue embryonic lethality of *Brca1*, *Bard1*, and *tsg101* mutant embryos (36–39). *Brca1*, *Bard1*, and *tsg101*-null embryos die approximately at E6.5 and E7.5, do not form mesoderm, and display decreased cell proliferation and elevated p53 expression. Disruption of the *p53* gene in these mutant embryos delays the embryonic lethality until E8.5–9.5. Like MetAP2, Brca1, Bard1, and tsg101 all have been implicated in the regulation of ubiquitin-mediated protein degradation (40–42). In addition, loss of function of the *BRCA1* or *BARD1* genes can cause genomic instability, which may up-regulate p53. At present, there is no direct evidence that loss of MetAP-2 function can lead to genomic instability. It is not yet known how p53 is up-regulated by loss of MetAP-2 activity, and how *p53* deletion rescues $MAP2^{D/D}$ phenotypes. We cannot rule out the possibility that p53 deficiency delays the apoptotic consequence in $MAP2^{D/D}$ embryos, although in *Brca1*, *Bard1*, and *tsg101*-null embryos, increased apoptosis is not detected. Thus, together, these results suggest that p53-induced growth arrest may act as a common checkpoint in embryonic development before gastrulation.

MetAP-2 Is Required for Endothelial Cell Proliferation. Two recent conflicting papers raise questions whether MetAP-2 is the physiological target of the Fg class of antiangiogenic compounds. In the first study (18), MetAP-2 protein levels were decreased by using RNAi; however, the resulting cells remained sensitive to Fg and other MetAP-2 inhibitors. In the second report (31), similar MetAP-2-targeted RNAi experiments resulted in decreased endothelial proliferation, suggesting an essential role for MetAP-2 in cell growth. Our RNAi results targeting MetAP-2 in endothelial cells corroborate the latter study. In addition, we show that HUVE cells expressing MetAP-2 shRNA are no longer sensitive to Fg-mediated cell cycle arrest. The discrepancy between our findings and the earlier RNAi studies of Kim *et al.* (18) may be due to our ability to achieve greater knockdown of MetAP-2 expression by targeting a different sequence of the MetAP-2 mRNA. Moreover, we were able to corroborate these RNAi results by using Cre-mediated excision of the *MAP2* gene in primary murine endothelial cells. Thus, given our two concurring independently derived results, we can conclude that MetAP-2 is the cytostatic target of Fg and that MetAP-2 function is required for endothelial cell proliferation.

Endothelial Expression of MetAP-2 Is Required for Vasculogenesis. Because vascular development cannot be analyzed in $MAP2^{D/D}$ mice because of their early gastrulation defect, we specifically excised *MAP2* from the developing hemangioblast line to study the effect of MetAP-2 deficiency on vasculogensis. The resulting lack of blood vessel development in these mice demonstrates the *in vivo* importance of MetAP-2 in normal vascular development and corroborates our findings that MetAP-2 knockdown results in endothelial growth arrest in cell culture. Our findings are also consistent with those seen in mice homozygous null for other genes (*VEGF* and *Flt-1*) required for angiogenesis (29, 30) and confirm previous studies showing a correlation between MetAP-2 function and angiogenesis (12).

Because of the early embryonic phenotypes of *MAP2*-null embryos, one may postulate that MetAP-2 is required globally for cell growth or survival. Thus, the requirement of MetAP-2 in vasculogenesis may not be specific. However, the *in vitro* outgrowth of *MAP2*-null blastocysts is not affected, which appears to be the major difference between *MAP2*-null embryonic phenotypes and the pregastrulation phenotypes observed in *Brca1*, *Bard1*, and *tsg101* mutant embryos (36, 37, 39). These data strongly suggest that MetAP-2 is not required for proliferation of embryonic cells *per se*, whereas we show that the growth of MetAP-2-deficient endothelial cells is greatly affected. In addition, it has been shown that of many cell types tested, endothelial cells are the most sensitive to the cytostatic inhibition of TNP-470 (10). It is not without precedent that a ubiquitously expressed protein infers tissue-specific function. For example, even though ubiquitous deletion of the cytoplasmic thioredoxin reductase gene (*Txnrd1*) results in early embryonic lethality, mice with a heart-specific inactivation of *Txnrd1* develop

normally (43). The full range of MetAP-2 function still remains to be tested, which may be done by generating tissue-specific or temporal-regulated *MAP2* knockout mice.

In summary, we report here the generation of *MAP2*-null ($MAP2^D$) and *MAP2* floxed ($MAP2^S$) mouse lines, which have permitted the study of MetAP-2 function in vertebrate development. These studies established a physiological role for MetAP-2 in early embryonic development as well as in a p53-dependent gastrulation checkpoint. Moreover, our results further support the conclusion that MetAP-2 is required for endothelial cell growth, and that MetAP-2 inhibition (i.e., by means of TNP-470) effectively disrupts vascular development. Notably, some adverse neurological effects of TNP-470 administration have been reported from clinical trials (44). It remains unclear whether these adverse effects are associated with MetAP-2 inhibition, although a recent TNP-470 derivative that is incapable of crossing the blood–brain barrier aims to minimize these effects (45). The conditional knockout mice reported here will undoubtedly prove useful in the exploration of the many phenotypes observed upon TNP-470 treatment as well as in the development of additional antiangiogenic and anticancer therapeutic agents.

Materials and Methods

Generation of *MetAP-2* Mutant Mice. A bacterial artificial chromosome (BAC) clone containing the *MAP2* gene was identified from a mouse ES-129/SvJ BAC library (Genome Systems, St. Louis) through PCR screening using primers designed according to the mouse *MAP2* cDNA sequence (MuKO5, 5′-AGGTGTATGCCATTGAGACC; MuKO7, 5′-GTATTACACAGGTCCACTGC). This clone was subsequently mapped and partially sequenced. To construct the *MAP2* targeting vector, a 6-kb BglII fragment containing both the first and the second exons of the *MAP2* gene was subcloned into pBluescript SK. Two loxP sites were then inserted into exon 1 before the translation start codon and in the first intron after exon 1. In addition, a neomycin-resistant gene flanked by two frt sequences was inserted into the first intron for drug selection. The vector was introduced into TC1 ES cells, and one targeting clone was obtained after screening 360 G418-resistant colonies. The recombination of the *MAP2* locus was confirmed by Southern blotting by using a 5′ probe for BglII or NcoI digestion and a 3′ probe for NcoI digestion.

Chimeric mice were generated by microinjection of the targeted ES cells into C57BL/6J blastocysts, and heterozygous germline-transmitted mice ($MAP2^{+/T}$) were successfully produced from crosses of the resulting highly chimeric males and C57BL/6 females. $MAP2^{+/T}$ mice were bred with *ACTB-Cre* transgenic mice (The Jackson Laboratory) to generate a *MAP2*-null mutation ($MAP2^{+/D}$). $MAP2^{+/T}$ mice have also been bred with *ACTB-Flp* transgenic mice (Gene Targeting Service, Yale University) to remove the neomycin gene in the intron and produce $MAP2^{+/S}$ mice. To generate a hemangioblast-specific *MAP2* mutant strain, $MAP2^{+/S}$ mice were crossed with *TIE2-Cre* transgenic mice (a gift from R. A. Flavell, Yale University). The Institutional Animal Care and Use Committee at Yale University approved all animal protocols used in this study.

shRNA Targeting Murine MetAP-2. Deoxyoligonucleotides encoding shRNA sequence against murine *MAP2* were synthesized at the Keck Biotechnology Center (Yale University School of Medicine). Sense oligonucleotide 5′- GATCCCCCAGTGGACCCATGTAATACTTCAAGAGAGTATTACATGGGTCCACTGTTTTTGGAAA-3′, and the antisense 5′-AGCTTTTCCAAAAACAGTGGACCCATGTAATACTCTCTTGAAGTATTACATGGGTCCACTGGGG-3′ were cloned into the BglII/HindIII sites of retrovirus pSUPER vector (OligoEngine, Seattle). Retrovirus containing shRNA sequence against murine *MAP2* was produced by using Pantropic Retroviral Expression System (Clontech) and used to infect MPE cells before selection with 1 μg/ml puromycin.

For more information on materials and methods, please see *Supporting Text*, which is published as supporting information on the PNAS web site.

We appreciate the many helpful discussions with Dr. Weimin Zhong. This work was supported by National Institutes of Health Grant CA083049 (to C.M.C.).

1. Sherman, F., Stewart, J. W. & Tsunasawa, S. (1985) *BioEssays* **3,** 27–31.
2. Arfin, S. M., Kendall, R. L., Hall, L., Weaver, L. H., Stewart, A. E., Matthews, B. W. & Bradshaw, R. A. (1995) *Proc. Natl. Acad. Sci. USA* **92,** 7714–7718.
3. Boutin, J. A. (1997) *Cell Signal.* **9,** 15–35.
4. Polevoda, B. & Sherman, F. (2002) *Genome Biol.* **3,** reviews0006.
5. Bachmair, A., Finley, D. & Varshavsky, A. (1986) *Science* **234,** 179–186.
6. Chang, S. Y., McGary, E. C. & Chang, S. (1989) *J. Bacteriol.* **171,** 4071–4072.
7. Li, X. & Chang, Y.-H. (1995) *Proc. Natl. Acad. Sci. USA* **92,** 12357–12361.
8. Sin, N., Meng, L., Wang, M. Q. W., Wen, J. J., Bornmann, W. G. & Crews, C. M. (1997) *Proc. Natl. Acad. Sci. USA* **94,** 6099–6103.
9. Griffith, E. C., Zhuang, S., Turk, B. E., Chen, S., Chang, Y.-H., Wu, Z., Biemann, K. & Liu, J. O. (1997) *Chem. Biol.* **4,** 461–471.
10. Kusaka, M., Sudo, K., Matsutani, E., Kozai, Y., Marui, S., Fujita, T., Ingber, D. & Folkman, J. (1994) *Br. J. Cancer* **69,** 212–216.
11. Bergers, G., Javaherian, K., Lo, K. M., Folkman, J. & Hanahan, D. (1999) *Science* **284,** 808–812.
12. Wang, J., Sheppard, G. S., Lou, P., Kawai, M., BaMaung, N., Erickson, S. A., Tucker-Garcia, L., Park, C., Bouska, J., Wang, Y. C., *et al.* (2003) *Cancer Res.* **63,** 7861–7869.
13. Bernier, S. G., Lazarus, D. D., Clark, E., Doyle, B., Labenski, M. T., Thompson, C. D., Westlin, W. F. & Hannig, G. (2004) *Proc. Natl. Acad. Sci. USA* **101,** 10768–10773.
14. Chun, E., Han, C. K., Yoon, J. H., Sim, T. B., Kim, Y. K. & Lee, K. Y. (2005) *Int. J. Cancer* **114,** 124–130.
15. Garrabrant, T., Tuman, R. W., Ludovici, D., Tominovich, R., Simoneaux, R. L., Galemmo, R. A., Jr., & Johnson, D. L. (2004) *Angiogenesis* **7,** 91–96.
16. Hannig, G., Lazarus, D. D., Bernier, S. G., Karp, R. M., Lorusso, J., Qiu, D., Labenski, M. T., Wakefield, J. D., Thompson, C. D. & Westlin, W. F. (2006) *Int. J. Oncol.* **28,** 955–963.
17. Brdlik, C. M. & Crews, C. M. (2004) *J. Biol. Chem.* **279,** 9475–9480.
18. Kim, S., LaMontagne, K., Sabio, M., Sharma, S., Versace, R. W., Yusuff, N. & Phillips, P. E. (2004) *Cancer Res.* **64,** 2984–2987.
19. Lewandoski, M., Meyers, E. N. & Martin, G. R. (1997) *Cold Spring Harbor. Symp. Quant. Biol.* **62,** 159–168.
20. Meyers, E. N., Lewandoski, M. & Martin, G. R. (1998) *Nat. Genet.* **18,** 136–141.
21. Wilkinson, D. G., Bhatt, S. & Herrmann, B. G. (1990) *Nature* **343,** 657–659.
22. Acampora, D., Mazan, S., Lallemand, Y., Avantaggiato, V., Maury, M., Simeone, A. & Brulet, P. (1995) *Development (Cambridge, U.K.)* **121,** 3279–3290.
23. Hogan, B. L., Blessing, M., Winnier, G. E., Suzuki, N. & Jones, C. M. (1994) *Dev. Suppl.* 53–60.
24. Pearce, J. J., Penny, G. & Rossant, J. (1999) *Dev. Biol.* **209,** 98–110.
25. Yeh, J. R., Mohan, R. & Crews, C. M. (2000) *Proc. Natl. Acad. Sci. USA* **97,** 12782–12787.
26. Zhang, Y., Griffith, E. C., Sage, J., Jacks, T. & Liu, J. O. (2000) *Proc. Natl. Acad. Sci. USA* **97,** 6427–6432.
27. Jacks, T., Remington, L., Williams, B. O., Schmitt, E. M., Halachmi, S., Bronson, R. T. & Weinberg, R. A. (1994) *Curr. Biol.* **4,** 1–7.
28. Dumont, D. J., Gradwohl, G., Fong, G. H., Puri, M. C., Gertsenstein, M., Auerbach, A. & Breitman, M. L. (1994) *Genes Dev.* **8,** 1897–1909.
29. Carmeliet, P., Ferreira, V., Breier, G., Pollefeyt, S., Kieckens, L., Gertsenstein, M., Fahrig, M., Vandenhoeck, A., Harpal, K., Eberhardt, C., *et al.* (1996) *Nature* **380,** 435–439.
30. Fong, G. H., Rossant, J., Gertsenstein, M. & Breitman, M. L. (1995) *Nature* **376,** 66–70.
31. Bernier, S. G., Taghizadeh, N., Thompson, C. D., Westlin, W. F. & Hannig, G. (2005) *J. Cell Biochem.* **95,** 1191–1203.
32. Turk, B. E., Griffith, E. C., Wolf, S., Biemann, K., Chang, Y. H. & Liu, J. O. (1999) *Chem. Biol.* **6,** 823–833.
33. Wang, J., Lou, P. & Henkin, J. (2000) *J. Cell Biochem.* **77,** 465–473.
34. Cutforth, T. & Gaul, U. (1999) *Mech. Dev.* **82,** 23–28.
35. Gong, Y., Mo, C. & Fraser, S. E. (2004) *Nature* **430,** 689–693.
36. Hakem, R., de la Pompa, J. L., Elia, A., Potter, J. & Mak, T. W. (1997) *Nat. Genet.* **16,** 298–302.
37. McCarthy, E. E., Celebi, J. T., Baer, R. & Ludwig, T. (2003) *Mol. Cell. Biol.* **23,** 5056–5063.
38. Hakem, R., de la Pompa, J. L., Sirard, C., Mo, R., Woo, M., Hakem, A., Wakeham, A., Potter, J., Reitmair, A., Billia, F., *et al.* (1996) *Cell* **85,** 1009–1023.
39. Ruland, J., Sirard, C., Elia, A., MacPherson, D., Wakeham, A., Li, L., de la Pompa, J. L., Cohen, S. N. & Mak, T. W. (2001) *Proc. Natl. Acad. Sci. USA* **98,** 1859–1864.
40. Chen, A., Kleiman, F. E., Manley, J. L., Ouchi, T. & Pan, Z. Q. (2002) *J. Biol. Chem.* **277,** 22085–22092.
41. Hashizume, R., Fukuda, M., Maeda, I., Nishikawa, H., Oyake, D., Yabuki, Y., Ogata, H. & Ohta, T. (2001) *J. Biol. Chem.* **276,** 14537–14540.
42. Ponting, C. P., Cai, Y. D. & Bork, P. (1997) *J. Mol. Med.* **75,** 467–469.
43. Jakupoglu, C., Przemeck, G. K., Schneider, M., Moreno, S. G., Mayr, N., Hatzopoulos, A. K., de Angelis, M. H., Wurst, W., Bornkamm, G. W., Brielmeier, M. & Conrad, M. (2005) *Mol. Cell. Biol.* **25,** 1980–1988.
44. Kruger, E. A. & Figg, W. D. (2000) *Exp. Opin. Invest. Drugs* **9,** 1383–1396.
45. Satchi-Fainaro, R., Mamluk, R., Wang, L., Short, S. M., Nagy, J. A., Feng, D., Dvorak, A. M., Dvorak, H. F., Puder, M., Mukhopadhyay, D. & Folkman, J. (2005) *Cancer Cell* **7,** 251–261.